

Non-Hermitian-skin-effect-enhanced dynamical robustness of topological end states in non-reciprocal Su-Schrieffer-Heeger models and the electrical circuit's simulation

Li-Jun Adrain Lang (郎利君),* Yijiao Weng (翁益娇), Yunhui Zhang (张云辉), Enhong Cheng (成恩宏), and Qixia Liang (梁绮霞)
Guangdong Provincial Key Laboratory of Quantum Engineering and Quantum Materials,
School of Physics and Telecommunication Engineering,
South China Normal University, Guangzhou 510006, China

(Dated: December 22, 2024)

For non-Hermitian quantum models, the dynamics is not apparently reflected by the static properties, such as the complex energy spectrum and the non-Hermitian topological invariant, because of the non-orthogonality of the right eigenvectors, non-unitarity of the time evolution, breakdown of the adiabatic theory, etc, but it is more realistic in experiments. Here, we pay attention to the dynamics of the non-reciprocal Su-Schrieffer-Heeger model under open boundary conditions, and find that the topological end state is more robust than its Hermitian counterpart, because the non-Hermitian skin effect can suppress the part leaking to the bulk sites. To observe this, we propose a classical electric circuit with only few passive inductors and capacitors, the mapping of which is established to the quantum model, and then simulate its dynamics. This work explains how the non-Hermitian skin effect enhances the robustness of the topological end state, and offers an easy way, via the classical electric circuit, of studying the non-reciprocal quantum dynamics, which may be extended to other non-Hermitian models.

I. INTRODUCTION

In our textbooks of quantum mechanics, e.g., in Ref.¹, the Hamiltonians must be Hermitian, required by the reality of the system's energy. In 1998, Bender and Boettcher² found that complex Hamiltonians with \mathcal{PT} symmetry can also bear the real energy spectra when the \mathcal{PT} symmetry of the eigenstates is not broken. Then, a theory of non-Hermitian quantum mechanics was established³, even for general non-Hermitian Hamiltonian. Along with the development of the experimental techniques, non-Hermitian Hamiltonians can be engineered in many experimental labs, especially in topological photonics^{4,5}; also, the effective Hamiltonian for open quantum systems is in general non-Hermitian⁶. Therefore, the relevant theoretical problems naturally emerge as the concerns of the theoretical physicists. Among them, the exotic non-Hermitian topological phenomena⁷ distinct from the Hermitian systems, e.g., \mathcal{PT} symmetry breaking^{2,8,9}, exceptional points^{10–16}, breakdown of the bulk-boundary correspondence of the Hermitian topological systems^{17–37}, etc, draw considerable attentions.

Many works^{17–37} tried to define the topology in non-Hermitian systems by proposing various definitions of topological invariants, and restore the bulk-boundary correspondence in non-Hermitian topological systems. Among them, based on the non-reciprocal Su-Schrieffer-Heeger (SSH) model, Yao *et al.*²⁶ found that the breakdown comes from the so-called “non-Hermitian skin effect” under open boundary conditions (OBCs) and established a “non-Bloch” theory to restore the bulk-boundary correspondence for this \mathcal{PT} symmetric non-Hermitian model. This effect was theoretically studied recently in different contexts^{38–44}, proposed to realize on various platforms^{45–47}, and observed in electrical-circuit^{48,49}, mechanical⁵⁰, photonic^{51,52}, and cold-atom⁵³

experiments.

However, the bulk-boundary correspondence principle and the various definitions of the topological invariants have an implicit prerequisite — adiabatic theorem⁵⁴, which breaks down in non-Hermitian dynamics due to the non-unitarity of the time-evolution⁵⁵. Therefore, many static topological properties, e.g., topological invariants and end/edge states, of non-Hermitian systems cannot be easily manipulated and observed. Compared with the static analysis, the dynamics is more straightforward for experiments^{51–53} to investigate the exotic properties of non-Hermitian systems, and may also help understand the dynamics of open quantum systems^{6,56}.

Moreover, although the large energy gaps can protect the topological end/edge states of the Hermitian model, part of the initial end/edge states will also leak to the bulk in dynamics due to the superposition with the bulk states. If the non-reciprocity-induced non-Hermitian skin effect can suppress the bulk part, it would be useful to enhance the robustness of the topological end/edge states, which may be usefully exploited in amplifiers^{57,58}, lasers^{59–66}, and other non-Hermitian photonic devices⁶⁷.

In this paper, we pay attention to the dynamics of the initial end state in topologically different regimes of the non-reciprocal SSH model, and find that the non-Hermitian skin effect indeed eliminates the bulk leakage and thus renders the non-Hermitian topological end state more robust than the Hermitian counterpart.

To demonstrate these dynamical phenomena, using the similar idea in Ref.⁴⁵, we also propose an LC electrical circuit to simulate the non-reciprocal SSH model. The electrical circuit platform has been proved in recent years to be an easy-manipulating, low-cost, but powerful simulators for some topological phenomena^{48,49,68–76}, but most of them focused on the driving schemes to study the resonance of the eigenstates^{48,49}. Here, we use the

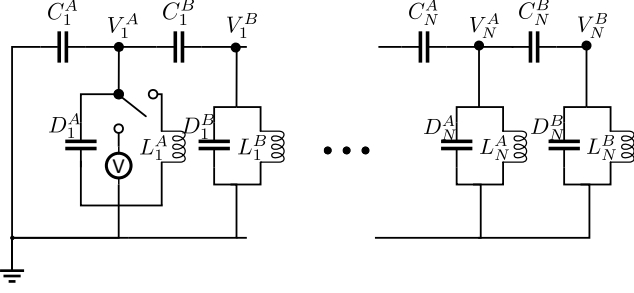


FIG. 3: The scheme of the electrical circuit to simulate the dynamics of the non-reciprocal SSH model, where the switch connects a DC voltage source to the left-most node for the initial state of the dynamics. Other parameters are defined in the text.

under the basis $|\psi\rangle$ in real space, where

$$\tilde{H} = S^{-1}HS = \begin{pmatrix} 0 & \nu & & & & \\ \nu & 0 & \kappa & & & \\ & \kappa & 0 & \nu & & \\ & & \ddots & \ddots & \ddots & \\ & & & \kappa & 0 & \nu \\ & & & & \nu & 0 \end{pmatrix} \quad (4)$$

is a $2N \times 2N$ Hermitian matrix, mathematically similar to H by an invertible matrix²⁶

$$S = \text{diag}(1, 1, e^{-\alpha}, e^{-\alpha}, \dots, e^{-(N-1)\alpha}, e^{-(N-1)\alpha}), \quad (5)$$

of which the exponentially decaying form is responsible for the non-Hermitian skin effect. The parameters $\kappa = \sqrt{\kappa_1 \kappa_2}$ and $\alpha = 2^{-1} \ln(\kappa_1/\kappa_2)$, where we assume that $\kappa_{1,2} > 0$ such that $\kappa, \alpha > 0$.

Focusing on Eq. (3), with the aid of the similarity transformation, the final state $\Psi(t)$ of H can be obtained from $\Psi(0)$ equivalently in three successive steps: (a) scaling by S^{-1} ; (b) evolving under the Hermitian matrix \tilde{H} ; (c) rescaling by S . Given an initial state confined in the left-most unit cell, $S^{-1}\Psi(0)$ in step (a) does not change it, preserving the signal only in the left-most unit cell. Then, the time-evolution in step (b) just follows the Hermitian case as mentioned before: depending on the parameters, transporting the signal into the bulk for the topologically trivial phase or keeping most signal in the left-most unit cell with small part transporting into the bulk for the topological phase. However, different from the Hermitian case, the rescaling S in step (c) eliminates exponentially the part leaking to the bulk.

IV. ELECTRICAL CIRCUIT'S FORMALISM OF THE NON-RECIPROCAL SSH MODEL

To simulate the fate of the initial end state in two topologically different phases of the non-reciprocal SSH model, we resort to LC electrical circuits, as shown in

Fig. 3, where we label the voltages of the A/B nodes in the n th unit cell as $V_n^{A/B}(t)$, the parameters $L_n^{A/B}$ as the corresponding inductances, and $C_n^{A/B}$ and $D_n^{A/B}$ as the capacitances.

We first do the static analysis, which corresponds to the switch in Fig. 3 connecting to the inductor. Assuming $V_n^{A/B}(t) = V_n^{A/B} e^{i\omega t}$, according to the Kirchoff's current law with the admittances of inductors and capacitors, i.e., $Y_L = 1/i\omega L$ and $Y_C = i\omega C$, where ω is the angular frequency, we have the following set of equations,

$$\begin{aligned} \left(\Lambda_n^A - \frac{1}{\omega^2}\right) V_n^A &= L_n^A C_n^A V_{n-1}^B + L_n^A C_n^B V_n^B, \\ \left(\Lambda_n^B - \frac{1}{\omega^2}\right) V_n^B &= L_n^B C_n^B V_n^A + L_n^B C_{n+1}^A V_{n+1}^A. \end{aligned} \quad (6)$$

where $\Lambda_n^A = L_n^A D_n^A + L_n^A C_n^A + L_n^A C_n^B$ and $\Lambda_n^B = L_n^B D_n^B + L_n^B C_n^B + L_n^B C_{n+1}^A$. We can also rewrite them in the matrix form, $\mathcal{H}\mathcal{V} = \mathcal{E}\mathcal{V}$, where $\mathcal{V} = (V_1^A, V_1^B, \dots, V_N^A, V_N^B)^T$,

$$\mathcal{H} = \begin{pmatrix} 0 & L_1^A C_1^B & & & \\ L_1^B C_1^B & 0 & L_1^B C_2^A & & \\ & \ddots & \ddots & \ddots & \\ & & L_N^A C_N^A & 0 & L_N^A C_N^B \\ & & & L_N^B C_N^B & 0 \end{pmatrix}, \quad (7)$$

and

$$\mathcal{E} = \Lambda - \frac{1}{\omega^2} I = \text{diag}(\Lambda_1^A, \Lambda_1^B, \dots, \Lambda_N^A, \Lambda_N^B) - \frac{1}{\omega^2} I, \quad (8)$$

where I is the identity matrix.

To map this set of equations to the non-reciprocal SSH model, we just regard \mathcal{H} as the Hamiltonian matrix H , \mathcal{V} and \mathcal{E} respectively as its right eigenvector and eigenenergy. Thus, $\mathcal{H}\mathcal{V} = \mathcal{E}\mathcal{V}$ can simulate the time-independent Schrödinger equation of the non-reciprocal SSH model if \mathcal{E} and thus Λ are proportional to the identity matrix.

To establish the mapping between the parameters of two Hamiltonian systems, Eqs. (2) and (7), we must have the following relations (in dimensionless way),

$$\begin{aligned} \frac{L_n^A C_n^B}{LC} &= \frac{L_n^B C_n^B}{LC} = 1, \\ \frac{L_n^B C_{n+1}^A}{LC} &= \frac{\kappa_1}{\nu}, \quad \frac{L_n^A C_n^A}{LC} = \frac{\kappa_2}{\nu}, \\ \frac{\Lambda_n^A}{LC} &= \frac{\Lambda_n^B}{LC} = \lambda, \quad (n = 1, \dots, N), \end{aligned} \quad (9)$$

where λ is a dimensionless constant taken as needed, and L and C are just reference parameters of inductors and capacitors, respectively, taken for practical need. The solution for the inductors and capacitors in the LC circuit

is as follows,

$$\begin{aligned} C_n^A &= C \left(\frac{\kappa_1}{\kappa_2} \right)^{n-1}, & C_n^B &= C_n^A \cdot \frac{\nu}{\kappa_2}, \\ D_n^A &= C_n^A \cdot \frac{\lambda\nu - \nu - \kappa_2}{\kappa_2}, & D_n^B &= C_n^A \cdot \frac{\lambda\nu - \nu - \kappa_1}{\kappa_2}, \\ L_n^A &= L_n^B = L \left(\frac{\kappa_2}{\kappa_1} \right)^{n-1} \cdot \frac{\kappa_2}{\nu}, & (n &= 1, \dots, N). \end{aligned} \quad (10)$$

Note that the inductances and the capacitances must be non-negative, which can be realized by setting $L, C > 0$ and $\lambda \geq 1 + \max(\kappa_1/\nu, \kappa_2/\nu)$, accompanied by the model parameters $\kappa_{1,2}, \nu > 0$ mentioned before. For convenience, we can set $\lambda = 1 + \kappa_1/\nu$ for the case of $\kappa_1 \geq \kappa_2$ to remove the inductances D_n^B in the circuit, i.e., $D_n^B = 0$, and thus, $D_n^A = C_n^A(\kappa_1 - \kappa_2)/\kappa_2$. In these settings, we have the effective Hamiltonian matrix $\mathcal{H} = (LC/\nu)H$ and the effective eigenenergy $\mathcal{E} = (\lambda LC - 1/\omega^2)I$.

We can also use another circuit scheme by just exchanging inductors and capacitors. The results can be easily obtained by the duality replacement: $\omega^2 \rightarrow 1/\omega^2$, $C_n^{A/B} \leftrightarrow 1/L_n^{A/B}$, $D_n^{A/B} \rightarrow 1/l_n^{A/B}$ in Eqs. (6), (7), and (10), where $l_n^{A/B}$ is another label of inductors.

V. ELECTRICAL CIRCUIT'S DYNAMICAL SIMULATION

For the dynamical simulation, we need consider the original differential equation, i.e.,

$$(\mathcal{H} - \Lambda)\ddot{\mathcal{V}}(t) - \mathcal{V}(t) = 0, \quad (11)$$

where \mathcal{H} and Λ are defined generally in Eqs. (7) and (8), and $\mathcal{V}(t) = [V_1^A(t), V_1^B(t), \dots, V_N^A(t), V_N^B(t)]^T$. The dot in $\dot{\mathcal{V}}$ means the derivative with respect to time, i.e., $d\mathcal{V}/dt$. Under the substitutions, Eqs. (9) or (10), the general solution reads

$$\mathcal{V}(t) = \sum_{n=1}^{2N} (\alpha_n \cos \omega_n t + \beta_n \sin \omega_n t) \cdot \mathcal{V}_n, \quad (12)$$

where \mathcal{V}_n is n th right eigenvector of \mathcal{H} , and ω_n is the corresponding eigen angular frequency of the circuit. $\{\alpha_n, \beta_n\}$ are a set of complex coefficients to be determined by the initial conditions, coming from the second order derivatives with respect to time in Eq. (11). The detailed derivation can be referred to in Appendix. The form of the superposition coefficients in Eq. (12) is different from our familiar form of the solution of the time-dependent Schrödinger equation, but it is qualitatively the same due to the same fact that the solution is the superposition of the Hamiltonian's eigenvectors.

To simulate the previously mentioned dynamics of the two topologically different phases, we adopt the LC circuit in Fig. 3. For the following selected values of parameters $(\kappa_1/\nu, \kappa_2/\nu, \lambda)$, we set the reference parameters in

Eq. (10) as $L = 1\text{mH}$ and $C = 100\text{pF}$, and the number of unit cells $N = 5$, which ensures that all values of circuit elements drop into the available regime in the realistic experiment. The typical oscillating angular frequency of the circuit is $\omega_0 = 1/\sqrt{LC}$ in the order of MHz.

For the topological phase, we choose $(\kappa_1/\nu, \kappa_2/\nu, \lambda) = (4, 1, 5)$ to simulate the dynamics of the non-reciprocal SSH model, corresponding to $C_n^A = C_n^B = 100\text{pF} \sim 25.6\text{nF}$, $D_n^A = 300\text{pF} \sim 76.8\text{nF}$, $D_n^B = 0$, and $L_n^A = L_n^B = 1\text{mH} \sim 3.9\mu\text{H}$; as comparison, we also choose $(\kappa_1/\nu, \kappa_2/\nu, \lambda) = (2, 2, 5)$ for the Hermitian counterpart, corresponding to $D_n^A = D_n^B = C_n^A = 100\text{pF}$, $C_n^B = 50\text{pF}$, and $L_n^A = L_n^B = 2\text{mH}$. Here, we use $n = 1, \dots, 5$. These two cases are said to be topological and have the topological end states because $|\kappa_1\kappa_2/\nu^2| = 4 > 1$.

For the topologically trivial phase, we choose $(\kappa_1/\nu, \kappa_2/\nu, \lambda) = (1, 0.25, 2)$, corresponding to $C_n^A = 100\text{pF} \sim 25.6\text{nF}$, $C_n^B = 400\text{pF} \sim 102.4\text{nF}$, $D_n^A = 300\text{pF} \sim 76.8\text{nF}$, $D_n^B = 0$, and $L_n^A = L_n^B = 250 \sim 1\mu\text{H}$; as comparison, we also choose $(\kappa_1/\nu, \kappa_2/\nu, \lambda) = (0.5, 0.5, 2)$ for the Hermitian counterpart, corresponding to $D_n^A = D_n^B = C_n^A = 100\text{pF}$, $C_n^B = 200\text{pF}$, and $L_n^A = L_n^B = 500\mu\text{H}$. They are topologically trivial and have no topological end states because $|\kappa_1\kappa_2/\nu^2| = 0.25 < 1$.

The initial state can be prepared by connecting the switch to the DC voltage source, and after a sufficient time, only capacitors C_1^A and C_1^B are charged, which renders only $V_1^A(0) = V_0$ with V_0 being the value of the DC voltage source, and thus determines the values of $\{\alpha_n\}$. By changing the switch to the inductor in 1st unit cell at time $t = 0$, the zero transient current renders $\dot{V}_n^{A/B} = 0$ for all n , and thus vanishes $\{\beta_n\}$. The determination of $\{\alpha_n, \beta_n\}$ can be referred to in Appendix. Then, $\mathcal{V}(t)$ of any time can be simulated according to Eq. (12).

Figure 4 shows the simulation results. As expected, compared with their Hermitian counterparts [Fig. 4(a) and 4(b)], we can clearly see that the non-reciprocity of both topological and topologically trivial cases can suppress the bulk leakage [Fig. 4(c) and 4(d)], and thus make the topological end state more robust. Figure 4(e) just confirms that the topological end state of the non-reciprocal SSH circuit is dynamically more localized than the Hermitian counterpart. Figure 4(d) also shows dynamically the non-Hermitian skin effect in the topologically trivial circuit, where the non-reciprocal state is accumulated to the left end, in opposite to the Hermitian counterpart, which spreads uniformly in the whole circuit.

To quantitatively reflect the extent of localization, we calculate the average inverse participation ratio (aIPR), defined as

$$\text{aIPR} = \frac{\sum_n \{[\bar{V}_n^A(t)]^4 + [\bar{V}_n^B(t)]^4\}}{\sum_n \{[\bar{V}_n^A(t)]^2 + [\bar{V}_n^B(t)]^2\}}, \quad (13)$$

where

$$\bar{V}_n^{A/B}(t) = \frac{2}{t} \int_{t/2}^t |V_n^{A/B}(\tau)| d\tau. \quad (14)$$

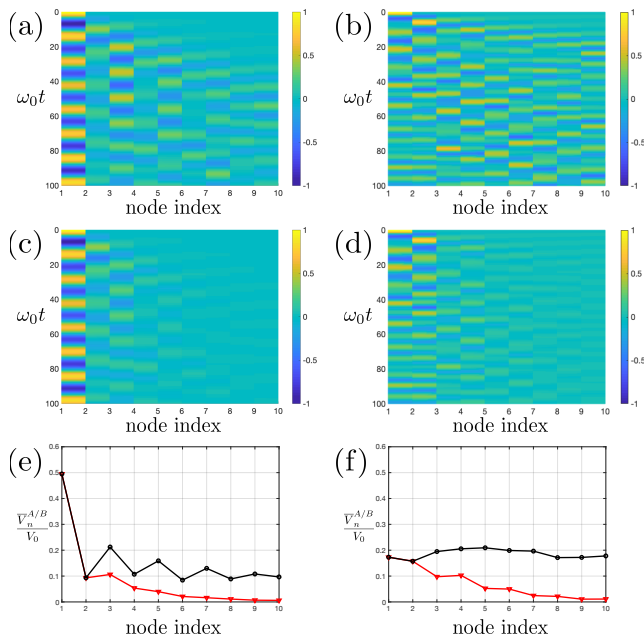


FIG. 4: Time evolution of the relative voltages, $V_n^{A/B}(t)/V_0$, in the circuit of Fig. 3, given the initial condition by the switch changing described in the main text, for the Hermitian SSH circuits with (a) $(\kappa_1/\nu, \kappa_2/\nu, \lambda) = (2, 2, 5)$ and (b) $(0.5, 0.5, 2)$, and for the non-reciprocal SSH circuits with (c) $(\kappa_1/\nu, \kappa_2/\nu, \lambda) = (4, 1, 5)$ and (d) $(1, 0.25, 2)$. (e,f) show the average voltages, $\bar{V}_n^{A/B}(t)/V_0$ (defined in the main text) at $\omega_0 t = 100$ for the (a,c) topological and (b,d) topologically trivial cases, where the non-reciprocal ones are labelled by the triangle (red) lines and the Hermitian ones by the circle (black) lines.

aIPR = 1 means that the averaged voltage distribution in the time interval $(t/2, t)$ is totally localized at one circuit node, while aIPR = $1/2N$ means the uniformly extended in the whole circuit. As the quantitative verification of the previous judgment, the aIPRs are equal to 0.8243 (red triangle) and 0.4209 (black circle) for the curves in Fig. 4(e), and 0.2611 (red triangle) and 0.1031 (black circle) in Fig. 4(f).

Actually, the dynamical behaviors in Fig. 4 can also be understood using the circuit's version of Eq. (3). To achieve this, we rewrite Eq. (11) into the form of a first order differential equation as follows,

$$\begin{pmatrix} \dot{\mathcal{V}}(t) \\ \dot{\mathcal{W}}(t) \end{pmatrix} = \begin{pmatrix} 0 & I \\ (\mathcal{H} - \Lambda)^{-1} & 0 \end{pmatrix} \begin{pmatrix} \mathcal{V}(t) \\ \mathcal{W}(t) \end{pmatrix} \quad (15)$$

by introducing $\mathcal{W}(t) = \dot{\mathcal{V}}(t)$ as new variables. And now, it is more like the time-dependent Schrödinger equation,

and the solution can be written as,

$$\begin{aligned} \begin{pmatrix} \mathcal{V}(t) \\ \mathcal{W}(t) \end{pmatrix} &= \exp \left[\begin{pmatrix} 0 & I \\ (\mathcal{H} - \Lambda)^{-1} & 0 \end{pmatrix} t \right] \cdot \begin{pmatrix} \mathcal{V}(0) \\ \mathcal{W}(0) \end{pmatrix} \\ &= \begin{pmatrix} S & 0 \\ 0 & S \end{pmatrix} \cdot \exp \left[\begin{pmatrix} 0 & I \\ (\tilde{\mathcal{H}} - \Lambda)^{-1} & 0 \end{pmatrix} t \right] \\ &\quad \cdot \begin{pmatrix} S^{-1} & 0 \\ 0 & S^{-1} \end{pmatrix} \begin{pmatrix} \mathcal{V}(0) \\ \mathcal{W}(0) \end{pmatrix}, \end{aligned} \quad (16)$$

where $\tilde{\mathcal{H}} = S^{-1}\mathcal{H}S$ is the Hermitian counterpart with S being defined in Eq. (5). This is qualitatively the same as Eq. (3), and thus, the same explanation also applies to the circuit SSH systems.

VI. CONCLUSION AND DISCUSSION

The non-reciprocal SSH model is fundamental to the understanding of the non-Hermitian physics. In this paper, we transfer the focus from the static properties to the direct dynamics, showing that the non-Hermitian skin effect of this model under OBCs can enhance the robustness of the dynamics of the topological end states with a succinct explanation. Then, we propose an electrical circuit with only few passive elements of linear inductors and capacitors to simulate the non-reciprocal SSH model, clearly demonstrating the advantage in dynamics over the Hermitian counterparts for the topological end states.

In this paper, we restrict the model parameters as $\kappa_{1,2}, \nu > 0$, which can be easily extended to $(\kappa_1/\nu)(\kappa_2/\nu) > 0$, showing the same dynamical properties, because the similarity transformation S still works to map it back to a Hermitian counterpart. However, for $(\kappa_1/\nu)(\kappa_2/\nu) < 0$, the eigenenergy or eigen angular frequency can in general be complex, and thus, the amplitude will be amplifying or decaying in time; furthermore, the circuit scheme with Eq. (10) cannot simulate this case due to the positivity of the circuit elements, which is beyond our discussion.

For experiments, the inductors and capacitors don't have to be selected with the exact values in the main text, because the non-Hermitian skin effect here just depends on the increasing or decreasing of the values, not the exact power law in Eq. (10). Therefore, the small intrinsic inductances and capacitances of the circuit cannot qualitatively affect the results either; so do the small resistances of the connecting wires in the circuit, which only quantitatively decays the amplitudes in a long time.

For the starting of the time evolution in circuit experiments, in principle the switching time must be much smaller than the discharging time of the capacitors to ensure the little change of the initial state at $t = 0$. Alternatively, we may consider the driving scheme to investigate the robustness of the non-reciprocal SSH end state as in Ref.⁴⁵, but it's another story.

Acknowledgments

This work was supported by the National Natural Science Foundation of China (11904109), Guangdong Basic and Applied Basic Research Foundation (2019A1515111101), and the startup funding from South China Normal University.

Dynamical solution of the electrical circuit

Under the substitutions, Eqs. (9) or (10), where note that $\Lambda = (\lambda LC)I$ is proportional to the identity matrix, we can make the following eigenvalue decomposition from Eqs. (7) and (8),

$$M^{-1}\mathcal{H}M = \mathcal{E} = \Lambda - (\Omega^2)^{-1}, \quad (17)$$

where the columns of M are just the $2N$ right eigenvectors of \mathcal{H} , i.e., $\{\mathcal{V}_n\}$, and $\Omega^2 = \text{diag}(\omega_1^2, \dots, \omega_{2N}^2)$ is the set of corresponding eigen angular frequencies of the circuit, $\{\omega_n\}$.

For the differential equation Eq. (11), applying the similarity transformation, Eq. (17), to both sides, we have

$$\begin{aligned} M^{-1}(\mathcal{H} - \Lambda)M[M^{-1}\dot{\mathcal{V}}(t)] - [M^{-1}\mathcal{V}(t)] &= 0 \\ \Rightarrow -(\Omega^2)^{-1}[M^{-1}\dot{\mathcal{V}}(t)] - M^{-1}\mathcal{V}(t) &= 0 \\ \Rightarrow [M^{-1}\dot{\mathcal{V}}(t)] + (\Omega^2)[M^{-1}\mathcal{V}(t)] &= 0. \end{aligned} \quad (18)$$

Because Ω^2 is a diagonal matrix, we can consider the solution for each element independently, i.e.,

$$\begin{aligned} [M^{-1}\mathcal{V}(t)]_n &= C_n e^{i\omega_n t} + D_n e^{-i\omega_n t} \\ &= \alpha_n \cos \omega_n t + \beta_n \sin \omega_n t, \end{aligned} \quad (19)$$

where $\{C_n, D_n\}$ and $\{\alpha_n = C_n + D_n, \beta_n = i(C_n - D_n)\}$ are two sets of complex coefficients to be determined by the initial conditions. Then, the final solution reads

$$\mathcal{V}(t) = MT(t), \quad (20)$$

where $T(t)$ is an $2N \times 1$ coefficient vector with entries $\{C_n e^{i\omega_n t} + D_n e^{-i\omega_n t}\}$ or $\{\alpha_n \cos \omega_n t + \beta_n \sin \omega_n t\}$. then we get the formula Eq. (12).

Given the initial conditions,

$$\begin{aligned} (\alpha_1, \dots, \alpha_{2N})^T &= T(0) = M^{-1}\mathcal{V}(0), \\ (\beta_1 \omega_1, \dots, \beta_{2N} \omega_{2N})^T &= \dot{T}(0) = M^{-1}\dot{\mathcal{V}}(0), \end{aligned} \quad (21)$$

the coefficients, say $\{\alpha_n, \beta_n\}$, can be determined, and thus, $\mathcal{V}(t)$ at any time is obtained.

-
- * Electronic address: ljiang@sncu.edu.cn
- ¹ J. J. Sakurai, *Modern Quantum Mechanics*, revised ed. (Addison-Wesley Publishing Company, 1994).
 - ² C. M. Bender and S. Boettcher, *Phys. Rev. Lett.* **80**, 5243 (1998).
 - ³ N. Moiseyev, *Non-Hermitian Quantum Mechanics*, 1st ed. (CAMBRIDGE UNIVERSITY PRESS, 2011).
 - ⁴ L. Lu, J. D. Joannopoulos, and M. Soljacic, *Nat Photon* **8**, 161004-1 (2014).
 - ⁵ T. Ozawa, H. M. Price, A. Amo, N. Goldman, M. Hafezi, L. Lu, M. C. Rechtsman, D. Schuster, J. Simon, O. Zeitlinger, and I. Carusotto, *Rev. Mod. Phys.* **91**, 015006 (2019).
 - ⁶ H.-P. Breuer and F. Petruccione, *THE THEORY OF OPEN QUANTUM SYSTEMS* (OXFORD UNIVERSITY PRESS, 2002).
 - ⁷ E. J. Bergholtz, J. C. Budich, and F. K. Kunst, arXiv:1912.10048 (2019).
 - ⁸ A. Guo, G. J. Salamo, D. Duchesne, R. Morandotti, M. Volatier-Ravat, V. Aimez, G. A. Siviloglou, and D. N. Christodoulides, *Phys. Rev. Lett.* **103**, 093902 (2009).
 - ⁹ B. Peng, S. K. Ozdemir, F. Lei, F. Monifi, M. Gianfreda, G. L. Long, S. Fan, F. Nori, C. M. Bender, and L. Yang, *Nature Physics* **10**, 394 (2014).
 - ¹⁰ B. Zhen, C. W. Hsu, Y. Igarashi, L. Lu, I. Kaminer, A. Pick, S.-L. Chua, J. D. Joannopoulos, and M. Soljacic, *Nature* **525**, 354 (2015).
 - ¹¹ K. Ding, G. Ma, M. Xiao, Z. Q. Zhang, and C. T. Chan, *Phys. Rev. X* **6**, 021007 (2016).
 - ¹² J. Doppler, A. A. Mailybaev, J. Bohm, U. Kuhl, A. Girschik, F. Libisch, T. J. Milburn, P. Rabl, N. Moiseyev, and S. Rotter, *Nature* **537**, 76 (2016).
 - ¹³ H. Xu, D. Mason, L. Jiang, and J. G. E. Harris, *Nature* **537**, 80 (2016).
 - ¹⁴ B. Midya, H. Zhao, and L. Feng, *Nature Communications* **9**, 2674 (2018).
 - ¹⁵ L. Jin, H. C. Wu, B.-B. Wei, and Z. Song, *Phys. Rev. B* **101**, 045130 (2020).
 - ¹⁶ S. M. Zhang, X. Z. Zhang, L. Jin, and Z. Song, *Phys. Rev. A* **101**, 033820 (2020).
 - ¹⁷ M. S. Rudner and L. S. Levitov, *Phys. Rev. Lett.* **102**, 065703 (2009).
 - ¹⁸ Y. C. Hu and T. L. Hughes, *Phys. Rev. B* **84**, 153101 (2011).
 - ¹⁹ K. Esaki, M. Sato, K. Hasebe, and M. Kohmoto, *Phys. Rev. B* **84**, 205128 (2011).
 - ²⁰ B. Zhu, R. Lü, and S. Chen, *Phys. Rev. A* **89**, 062102 (2014).
 - ²¹ T. E. Lee, *Phys. Rev. Lett.* **116**, 133903 (2016).
 - ²² D. Leykam, K. Y. Bliokh, C. Huang, Y. D. Chong, and F. Nori, *Phys. Rev. Lett.* **118**, 040401 (2017).
 - ²³ H. Shen, B. Zhen, and L. Fu, *Phys. Rev. Lett.* **120**, 146402 (2018).
 - ²⁴ S. Lieu, *Phys. Rev. B* **97**, 045106 (2018).

- ²⁵ C. Yin, H. Jiang, L. Li, R. Lü, and S. Chen, *Phys. Rev. A* **97**, 052115 (2018).
- ²⁶ S. Yao and Z. Wang, *Phys. Rev. Lett.* **121**, 086803 (2018).
- ²⁷ Y. Xiong, *Journal of Physics Communications* **2**, 035043 (2018).
- ²⁸ F. K. Kunst, E. Edvardsson, J. C. Budich, and E. J. Bergholtz, *Phys. Rev. Lett.* **121**, 026808 (2018).
- ²⁹ V. M. Martinez Alvarez, J. E. Barrios Vargas, and L. E. F. Foa Torres, *Phys. Rev. B* **97**, 121401 (2018).
- ³⁰ Z. Gong, Y. Ashida, K. Kawabata, K. Takasan, S. Higashikawa, and M. Ueda, *Phys. Rev. X* **8**, 031079 (2018).
- ³¹ S. Yao, F. Song, and Z. Wang, *Phys. Rev. Lett.* **121**, 136802 (2018).
- ³² L. Jin and Z. Song, *Phys. Rev. B* **99**, 081103 (2019).
- ³³ K. Kawabata, K. Shiozaki, and M. Ueda, *Phys. Rev. B* **98**, 165148 (2018).
- ³⁴ C. H. Lee, L. Li, and J. Gong, (2018).
- ³⁵ L.-J. Lang, Y. Wang, H. Wang, and Y. D. Chong, *Phys. Rev. B* **98**, 094307 (2018).
- ³⁶ H. Jiang, C. Yang, and S. Chen, *Phys. Rev. A* **98**, 052116 (2018).
- ³⁷ F. Song, S. Yao, and Z. Wang, *Phys. Rev. Lett.* **123**, 246801 (2019).
- ³⁸ C. H. Lee and R. Thomale, *Phys. Rev. B* **99**, 201103 (2019).
- ³⁹ C. H. Lee, L. Li, and J. Gong, *Phys. Rev. Lett.* **123**, 016805 (2019).
- ⁴⁰ L. Li, C. H. Lee, S. Mu, and J. Gong, arXiv:2003.03039 (2020).
- ⁴¹ T. Li, Y.-S. Zhang, and W. Yi, arXiv:2005.09474 (2020).
- ⁴² C. H. Lee, arXiv:2006.01182 (2020).
- ⁴³ J. Claes and T. L. Hughes, arXiv:2007.03738 (2020).
- ⁴⁴ K. Yang, S. C. Morampudi, and E. J. Bergholtz, arXiv:2007.04329 (2020).
- ⁴⁵ H. Jiang, L.-J. Lang, C. Yang, S.-L. Zhu, and S. Chen, *Phys. Rev. B* **100**, 054301 (2019).
- ⁴⁶ T. Hofmann, T. Helbig, C. H. Lee, M. Greiter, and R. Thomale, *Phys. Rev. Lett.* **122**, 247702 (2019).
- ⁴⁷ L. Li, C. H. Lee, and J. Gong, *Phys. Rev. Lett.* **124**, 250402 (2020).
- ⁴⁸ T. Helbig, T. Hofmann, S. Imhof, M. Abdelghany, T. Kiessling, L. W. Molenkamp, C. H. Lee, A. Szameit, M. Greiter, and R. Thomale, *Nature Physics* **16**, 747 (2020).
- ⁴⁹ T. Hofmann, T. Helbig, F. Schindler, N. Salgo, M. Brzezińska, M. Greiter, T. Kiessling, D. Wolf, A. Vollhardt, A. Kabaši, C. H. Lee, A. Bilušić, R. Thomale, and T. Neupert, *Phys. Rev. Research* **2**, 023265 (2020).
- ⁵⁰ A. Ghatak, M. Brandenbourger, J. van Wezel, and C. Coulais, arXiv:1907.11619 (2019).
- ⁵¹ L. Xiao, T. Deng, K. Wang, G. Zhu, Z. Wang, W. Yi, and P. Xue, *Nature Physics* **16**, 761 (2020).
- ⁵² S. Weidemann, P. Kremer, T. Helbig, T. Hofmann, A. Stegmaier, M. Greiter, R. Thomale, and A. Szameit, *Science* **368**(6488), 311 (2020).
- ⁵³ W. Gou, T. Chen, D. Xie, T. Xiao, T.-S. Deng, B. Gadway, W. Yi, and B. Yan, *Phys. Rev. Lett.* **124**, 070402 (2020).
- ⁵⁴ D. Xiao, M.-C. Chang, and Q. Niu, *Rev. Mod. Phys.* **82**, 110608-1 (2010).
- ⁵⁵ H. Wang, L.-J. Lang, and Y. D. Chong, *Phys. Rev. A* **98**, 012119 (2018).
- ⁵⁶ F. Song, S. Yao, and Z. Wang, *Phys. Rev. Lett.* **123**, 170401 (2019).
- ⁵⁷ G. Q. Liang and Y. D. Chong, *Phys. Rev. Lett.* **110**, 203904 (2013).
- ⁵⁸ V. Peano, M. Houde, F. Marquardt, and A. A. Clerk, *Phys. Rev. X* **6**, 041026 (2016).
- ⁵⁹ H. Schomerus, *Opt. Lett.* **38**, 1912 (2013).
- ⁶⁰ P. St-Jean, V. Goblot, E. Galopin, A. Lemaitre, T. Ozawa, L. Le Gratiet, I. Sagnes, J. Bloch, and A. Amo, *Nature Photonics* **11**, 651 (2017).
- ⁶¹ S. Malzard and H. Schomerus, *New Journal of Physics* **20**, 063044 (2018).
- ⁶² R. Yao, H. Li, B. Zheng, S. An, J. Ding, C.-S. Lee, H. Zhang, and W. Guo, arXiv:1804.01587 (2018).
- ⁶³ H. Zhao, P. Miao, M. H. Teimourpour, S. Malzard, R. El-Ganainy, H. Schomerus, and L. Feng, *Nature Communications* **9**, 981 (2018).
- ⁶⁴ M. A. Bandres, S. Wittek, G. Harari, M. Parto, J. Ren, M. Segev, D. N. Christodoulides, and M. Khajavikhan, *Science* **359**, eaar4005 (2018).
- ⁶⁵ G. Harari, M. A. Bandres, Y. Lumer, M. C. Rechtsman, Y. D. Chong, M. Khajavikhan, D. N. Christodoulides, and M. Segev, *Science* **359**, eaar4003 (2018).
- ⁶⁶ M. Parto, S. Wittek, H. Hodaei, G. Harari, M. A. Bandres, J. Ren, M. C. Rechtsman, M. Segev, D. N. Christodoulides, and M. Khajavikhan, *Phys. Rev. Lett.* **120**, 113901 (2018).
- ⁶⁷ D. Leykam and L. Yuan, arXiv:2007.11807 (2020).
- ⁶⁸ J. Ningyuan, C. Owens, A. Sommer, D. Schuster, and J. Simon, *Phys. Rev. X* **5**, 021031 (2015).
- ⁶⁹ C. H. Lee, S. Imhof, C. Berger, F. Bayer, J. Brehm, L. W. Molenkamp, T. Kiessling, and R. Thomale, *Communications Physics* **1**, 39 (2018).
- ⁷⁰ S. Imhof, C. Berger, F. Bayer, J. Brehm, L. W. Molenkamp, T. Kiessling, F. Schindler, C. H. Lee, M. Greiter, T. Neupert, and R. Thomale, *Nature Physics* **14**, 925 (2018).
- ⁷¹ Y. Hadad, J. C. Soric, A. B. Khanikaev, and A. Alu, *Nature Electronics* **1**, 178 (2018).
- ⁷² Y. Li, Y. Sun, W. Zhu, Z. Guo, J. Jiang, T. Kariyado, H. Chen, and X. Hu, *Nature Communications* **9**, 4598 (2018).
- ⁷³ K. Luo, R. Yu, and H. Weng, *Research* **2018**, 10 (2018).
- ⁷⁴ Y. Wang, L.-J. Lang, C. H. Lee, B. Zhang, and Y. D. Chong, *Nature Communications* **10**, 1102 (2019).
- ⁷⁵ Y. Lu, N. Jia, L. Su, C. Owens, G. Juzeliūnas, D. I. Schuster, and J. Simon, *Phys. Rev. B* **99**, 020302 (2019).
- ⁷⁶ M. Serra-Garcia, R. Süsstrunk, and S. D. Huber, *Phys. Rev. B* **99**, 020304 (2019).
- ⁷⁷ D.-W. Zhang, Y.-Q. Zhu, Y. X. Zhao, H. Yan, and S.-L. Zhu, *Advances in Physics* **67**, 253 (2018).
- ⁷⁸ X. Gu, A. F. Kockum, A. Miranowicz, Y.-x. Liu, and F. Nori, *Physics Reports* **718-719**, 1 (2017).
- ⁷⁹ W. P. Su, J. R. Schrieffer, and A. J. Heeger, *Phys. Rev. Lett.* **42**, 1698 (1979).